Applied Surface Science 255 (2009) 5532–5536

Contents lists available at ScienceDirect

Applied Surface Science

journal homepage: www.elsevier.com/locate/apsusc

Optimization of a laser mitigation process in damaged fused silica

S. Palmier [a,*], L. Gallais [a], M. Commandré [a], P. Cormont [b], R. Courchinoux [b], L. Lamaignère [b], J.L. Rullier [b], P. Legros [c]

[a] Institut Fresnel, CNRS, Ecole Centrale Marseille, Université Aix-Marseille, av. Escadrille Normandie 13397 Marseille Cedex 20, France
[b] CEA, CESTA, BP 2, 33114 Le Barp, France
[c] Plate-forme d'Imagerie Cellulaire, Institut François Magendie, 146 Rue Léo-Saignat, 33077 Bordeaux, France

ARTICLE INFO

Article history:
Available online 6 August 2008

PACS:
42.79.−e
42.70.Ce
81.65.−b

Keywords:
Laser mitigation process
Silica
Laser-induced damage

ABSTRACT

One of the major concerns encountered in high power laser is the laser-induced damage of optical components. This is a main issue of the development of the Europe's biggest laser, known as Laser Méga Joule (LMJ) especially in the section where the beam wavelength is 351 nm. This study deals with the development of a laser treatment process to improve the laser damage resistance of silica optical components. First, by irradiating the component at 355 nm in the nanosecond regime, defects of the silica optic are revealed and evolve as damage. Next, the damaged sites are irradiated with a CO_2 laser at a 10.6 μm wavelength in order to melt and evaporate the silica in the damage neighborhood. In this study, we performed a variation of the CO_2 laser parameters to obtain the most efficient stabilization. To check this stabilization, damage resistance tests were performed with an UV laser representative of the LMJ (at 355 nm/2.5 ns). The results show that we can stabilize weak points and thereby make the component resistant to subsequent UV laser irradiation.

1. Introduction

The French Atomic Energy Commission (CEA) has started to build the Europe's biggest laser, known as Laser Méga Joule (LMJ) [1]. LMJ will consist of 30 bundles, each containing eight laser beams, and will deliver a total energy of 1.8 MJ with a pulse length of a few nanoseconds. The 240 beams will be focused onto micron-sized targets containing deuterium and tritium to initiate a thermonuclear fusion reaction. A prototype installation at scale 1 of the future LMJ, called the Ligne d'Intégration Laser (LIL), has been working for a few years [2]. It is intended to validate technological choices made for LMJ and to prepare its exploitation. The LIL consists of a complete laser bundle of 8 beamlines. Each laser beam of 40 cm × 40 cm section is amplified at 1053 nm wavelength with pulses of duration a few nanoseconds. This wavelength is converted to 351 nm to be focused onto micron-sized targets. One of the major concerns encountered in the LIL exploitation is laser-induced damage of optical components [3], especially in the section where the beam wavelength is 351 nm. Although the polishing techniques of optical components have been considerably improved, defects that can initiate damage are still present in the material. Laser irradiations of these weak points lead to stress, cracks and absorption. The created damage growths under subsequent irradiations and makes the component unsuitable. The problem is that we still cannot predict why, when and where an optical component will be damaged. Because of the huge numbers, the large dimensions and the cost of optics present in the laser, it is impossible to plan to change them regularly. To avoid that, a process to improve the laser damage resistance was developed to be applied before the optics installation on line. This process, that we called stabilization, consists in finding the defects and mitigating their subsequent growth. To find defects, we irradiate the component with a table-top laser whose characteristics are comparable with LMJ beam parameters. After this step has been carried out, all sensitive zones have been damaged. The mitigation of damage growth is the most critical step. Several methods were tested on silica [4,5]: chemical treatment of the surface, the microwave or radio-frequency generated plasma etching, the laser or the micro-flame torch processing. One of the most promising methods consists in using a CO_2 laser operating at a 10.6 μm wavelength [6,7] to locally melt and evaporate the silica surface by producing typically smooth, Gaussian shaped pits [8–10]. This process has been used to polish silica and to increase the laser damage resistance [11–13] by reducing defects on surface [14]. A technique capable of controlling the melting of silica was developed by Mendez et al. to repair damage caused in the surface

* Corresponding author. Tel.: +33 4 91 28 83 93; fax: +33 4 91 28 80 67.
E-mail address: stephanie.palmier@fresnel.fr (S. Palmier).

0169-4332/$ – see front matter © 2008 Elsevier B.V. All rights reserved.
doi:10.1016/j.apsusc.2008.07.178

of mirrors without any mass loss [15]. For our applications, a process capable to treat deep damage is needed and this stabilized site has to withstand the 351 nm, 3 ns beam power in operating conditions.

In Section 2, the method and the experimental set-up developed for this aim are presented. In Section 3, a variation of the CO_2 laser irradiation parameters is performed in order to obtain the most efficient process capable to mitigate deep silica damages. In Section 4, these last results are compared to calculations and discussed. In Section 5, we analyze the laser damage resistance of stabilized area and discuss the efficiency of the process.

2. Experimental tools

An experimental set-up has been developed to stabilize fused silica (Fig. 1). It allows the visualization of damage sites on samples and their localized irradiation by a CO_2 laser. The energy deposition of the laser can be easily varied (beam focus size, mean power, maximum power, and pulse length). The laser (Synrad Firestar V20) operates at a 10.6 μm wavelength with a 20 W maximum power. Power control is achieved by pulsed width modulation at a 5 kHz frequency: a duty cycle of 10% corresponds to a power of 2 W and 100% to 20 W. The beam power is adjusted by two polarizers. A laser diode, which emits at 650 nm, is used to align the optics and to center the zone of the substrate to treat. A phase mirror changes the linear polarization of the CO_2 laser into a circular polarization for optical isolation and to get symmetric craters. The beam is focused with a ZnSe lens with a 10 in. focal length. The latter is mounted on a z translation stage to adjust the beam diameter on the sample from 200 μm to 800 μm measured at $1/e^2$. The sample is mounted on an x, y translation stage to select the zone to stabilize. The latter is observed by a microscope with a 50× to a 500× magnification objectives in bright and dark field mode. The dark field is particularly useful to observe debris deposit on the surface during the process. Different diagnostics in the laser path measure its power, and its temporal or spatial profile. The operation is assisted by computer.

Under irradiation a circular crater is created on the silica surface, whose size depends on the laser parameters. The dimensional characteristics of each crater are measured with a surface profiler (Talysurf CCI 300 nm) and a Nomarski microscope (Carl Zeiss Axiotech microscope).

Laser damage resistance tests are performed with a table-top laser, whose main characteristics are comparable with the LMJ/LIL laser beams. The laser used is a Nd:YAG which delivers a pulse length of 2.5 ns at 355 nm with a 10 Hz repetition rate. The laser beam is focused by a 5 m focal length lens to get a Gaussian spatial profile with a diameter of 0.9 mm at $1/e^2$. Damages are detected *in situ* with a mobile macroscope.

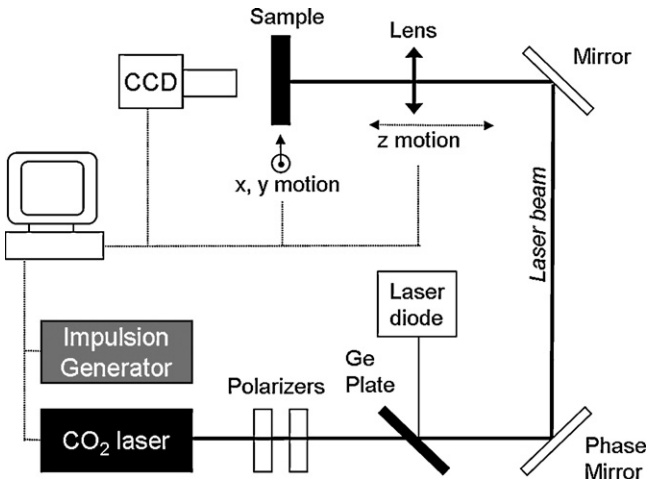

Fig. 1. Experimental set up.

3. Parametric study

As it has been observed in several studies, after an irradiation at a 351 nm wavelength with a few nanosecond pulse length and the nominal fluence of LMJ, typical damages are 15 μm deep and cracks can propagate up to a 20 μm depth [16–18]. Therefore, the best stabilization conditions correspond to the formation of a 20 μm deep crater in order to remove any offending material and make the surface area smooth and crackfree. To obtain it, the influence on the crater morphology of different CO_2 laser parameters such as the diameter, the laser pulse length and the power have to be studied.

This study has been carried out on a bare Heraeus S312 super-polished fused silica substrate of 50-mm diameter and 5-mm thickness. In a first experiment, the pulse length influence is analyzed. The beam diameter and the power were respectively set at 200 μm and 1.25 W. On each crater, the depth and the diameter are measured and found reproducible among the 15 craters obtained with the same parameters. From these experimental results, the depth and the diameter are plotted as functions of the pulse length in Fig. 2. For pulse lengths <0.25 s, the crater diameter remains stable at 70 μm and the depth increases linearly with the time. For pulse lengths >0.25 s, the diameter increases slowly with the time and the depth approaches a constant value. To explore these two behaviors, we chose to work with the pulse lengths of 0.25 s and 1 s.

In a second experiment, to get a 20-μm deep crater with these pulse lengths, the power and the diameter vary and their influence was analyzed. During this step, most of craters created with a high power and a small diameter are characterized by the presence of debris all around. This may evolve into new surface defects capable of initiating more damages. To avoid that, the power and the diameter are changed simultaneously. In Fig. 3, the crater depth and the diameter are represented as functions of the power; the corresponding CO_2 laser beam diameter is indicated in Fig. 3a. The crater diameter increases linearly with the power following the CO_2 laser beam diameter increase and independently of the pulse length (Fig. 3a). For power >2 W (and a beam diameter of 300 μm, 450 μm or 550 μm), the crater depth obtained with a 1 s pulse length is much higher than 20 μm (Fig. 3b) while the craters obtained with a 0.25 s pulse length are slightly higher than 20 μm. From this parametric study, we show that to get a crater whose depth exceeds 20 μm, different sets of irradiating conditions may be used.

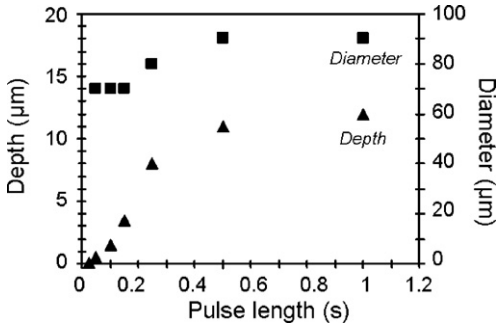

Fig. 2. Measured diameter and depth as a function of the pulse length (200 μm at $1/e^2$, 1.25 W).

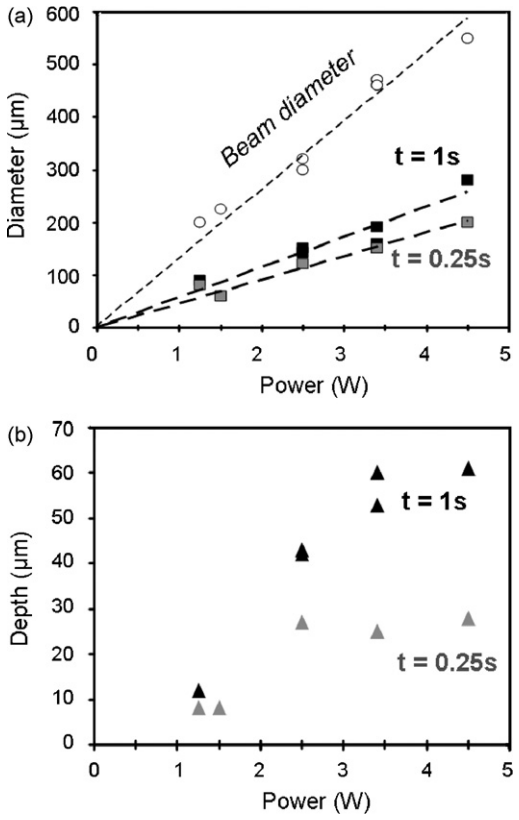

Fig. 3. Measured diameter (a) and depth (b) as a function of power for a 0.25 s (in grey) and 1 s (in black) pulse length.

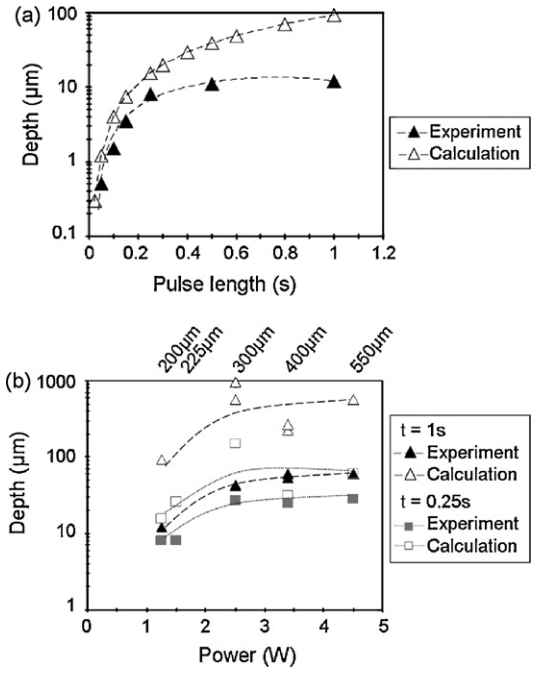

Fig. 4. Calculated and measured depth of removed silica as a function of the pulse length (a) and the beam power for the corresponding beam diameter (b).

4. Comparison between experiment and calculations

To complete this parametric study, some calculations based on the works of Feit and Rubenchik [9] were performed. We consider a Gaussian laser beam whose radius at $1/e^2$ is noted a. For a flat top temporal pulse with a constant intensity, I, the temperature increase at the centre of the laser spot, ΔT, is given by Eq. (1) [19]:

$$\Delta T = \frac{AP}{(\pi)^{3/2} a\kappa} \mathrm{Arc\,tan}\left(\sqrt{\frac{t}{\tau}}\right) \quad \text{with} \quad \tau = \frac{a^2}{4D} \tag{1}$$

where A is the absorbed fraction, $A = 0.85$ for fused silica irradiated at a 10.6 µm, $P = I\pi a^2$ is the beam power, D is the thermal diffusivity, $D = 8.34 \times 10^{-7}$ m^2/s, κ is the thermal conduction coefficient, $\kappa = 1.38$ W/(m K), and t is the time. These values represent typical data at 20 °C [20]. By knowing the temperature evolution, we can deduce the velocity of silica evaporation which is given by the following expression:

$$V = V_0\, \mathrm{e}^{-U/k\Delta T} \tag{2}$$

where U is the latent heat of evaporation per atom, $U = 3.6$ eV for fused silica and $V_0 = 3.8 \times 10^5$ cm/s.

Finally, the depth of removed material is given by the following equation:

$$d = \int V\, \mathrm{d}t \tag{3}$$

where d is the crater depth.

The calculated and the measured depth of removed silica are compared in Fig. 4 as functions of the pulse length and the beam power. In Fig. 4a, the results of calculations follow the same trend than the measured depth and good agreement is found for pulse length <0.25 s. But for longer pulse lengths, the difference between experiment and calculation increases with time. This difference, even more obvious in Fig. 4b, is more sensitive to pulse length variation than power variation.

These basic calculations do not consider any evolution of the silica properties with the temperature increase. Indeed, the thermal conductivity, the heat capacity, the refraction index and the coefficient of absorption become more important with temperature. For instance, a thermal conductivity of 1.38 W/(m K) at 20 °C achieves 2.68 W/(m K) at 900 °C. As Feit and Rubenchik discussed in Ref. [9], to take into account these variations will reduce the ablation rate will make the process be less sensitive to variation of the CO_2 laser parameters. For more fundamental understanding of the process, a more complete calculation has to be performed.

5. Damage resistance tests

After having discovered how to obtain 20 µm deep craters, we proceeded to analyze the resistance to damage of the stabilized silica under typical LMJ irradiation (351 nm, 3 ns, with a 10 J/cm^2 maximum fluence). Damage sites were created with a Nd:YAG laser with a 355 nm wavelength, a 2.5 ns pulse length, a 0.9 mm diameter and a fluence = 12 J/cm^2. The damage sites were then treated by a CO_2 laser irradiation with the six sets of parameters that create craters deeper than 20 µm. Fifteen craters were made with each set of CO_2 laser parameters. Each stabilized site was then irradiated by the same Nd:YAG. The test protocol consists of 100 shots at 8 J/cm^2, followed by 100 more at 11 J/cm^2, and finishing with 100 shots at 13 J/cm^2. If damage occurs after a shot, the test on that site is stopped, and the procedure is repeated on the next site. Each crater was observed by optical microscopy before and after the Nd:YAG laser irradiations.

Whatever the CO_2 laser parameters, three kinds of behavior were observed. Fig. 5 shows them: before mitigation, after mitigation by CO_2 laser irradiation, and after a typical LMJ

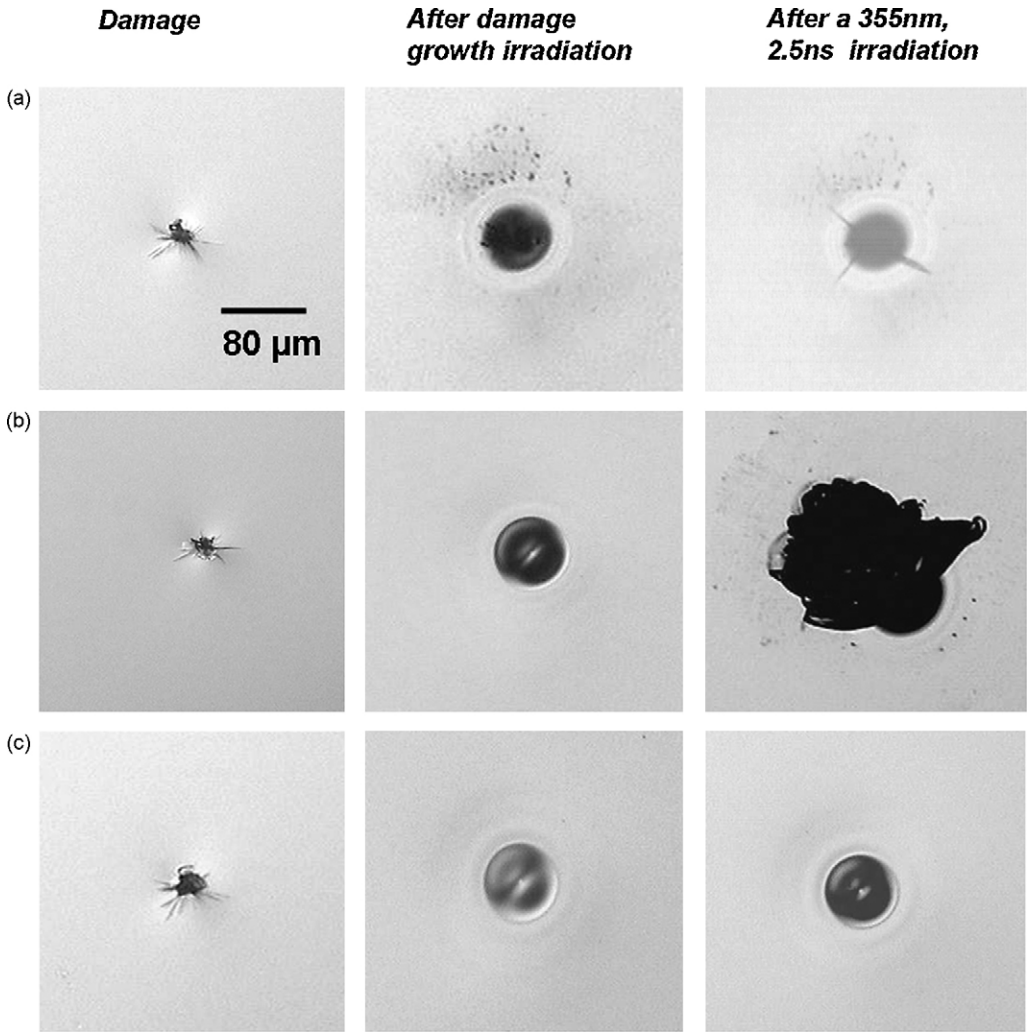

Fig. 5. Damages observed before mitigation, after mitigation and after an irradiation at a 355 nm wavelength and a 2.5 ns pulse length.

irradiation. In Fig. 5a, the stabilization crater was not deep enough to remove all the damaged silica and after one irradiation at 8 J/cm^2, three big fractures propagate from the previous damage. Some fractures generated by the damage were not mended in the silica melting and so the non-stabilized part of the damage continues to grow under irradiation. In Fig. 5b, the damage seems to have been removed, but after an 8 J/cm^2 irradiation, a large damage appears. In Fig. 5c, the crater does not evolve even after 100 irradiations at 13 J/cm^2. We consider this case a success.

A statistical study of the crater damage resistance was performed. The successful stabilizations after 8 J/cm^2, then at 11 J/cm^2 or 13 J/cm^2 irradiations were counted. The percentages of craters without damage are determined and represented in Fig. 6 as a function of the CO_2 laser parameters. The measured crater depth is also indicated. All the craters obtained with a CO_2 laser irradiation whose pulse length is 1 s are damaged after 8 J/cm^2 irradiations. These craters are also the deepest ones so the damage resistance may be linked with the depth or the pulse length. All the craters obtained with a 0.25 s CO_2 laser pulse have the same depth. Very good results are obtained for two kinds of craters with more than 80% of resistant sites to 100 irradiations at 11 J/cm^2. But the crater created with the parameters, 2.5 W, 0.25 s, 300 µm seems too small in comparison with its depth to withstand typical LMJ irradiations.

To explain why certain crater withstand typical LMJ irradiations and others not, residual stress in the heated silica could be considered [21,22]. We assume that during the CO_2 laser irradiation, silica surface is heated, melted, and bent. At the end of the CO_2 laser pulse, the silica cools down and becomes taut thus

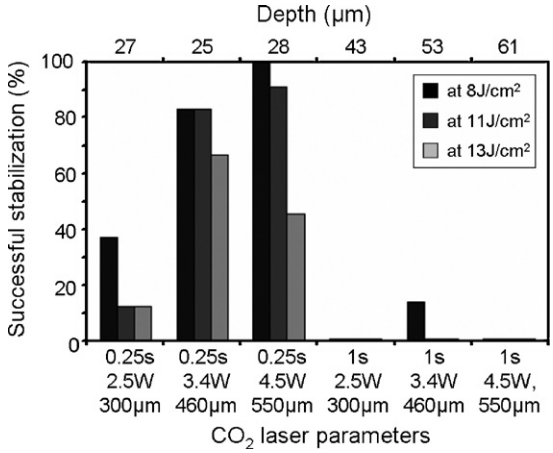

Fig. 6. Percentage of successful stabilization after 100 irradiations at 8 J/cm^2, at 11 J/cm^2 and 13 J/cm^2 with a wavelength of 355 nm and a pulse length of 2.5 ns.

creating stress in the material. The different parameters of irradiation induce amounts of residual stress, which is an important factor in the resistance of the site.

6. Conclusion

To stabilize optical components, a set-up has been developed and was successfully used. At present, typical damage initiated in silica components with comparable LMJ operating conditions are 20 μm deep. Thanks to our parametric study, several sets of CO_2 laser parameters were found to produce a crater deep enough to remove the damaged silica. But the necessity of laser damage resistance limits this parameter range. Suitable parameters were found to get a process to treat deep damage and to make silica withstand typical LMJ irradiations. Thus this efficient process can be used on real optical components before coating. However, further studies are needed to understand the behavior of the stabilized area.

References

[1] A. Bettinger, M. Decroisette, Fusion Eng. 46 (1999) 457.
[2] P. Eyharts, J.M. Di-Nicola, C. Féral, E. Germain, H. Graillot, F. Jequier, E. Journot, X. Julien, M. Luttmann, O. Lutz, G. Thiell, J. Phys. IV 133 (2006) 727.
[3] H. Bercegol, P. Bouchut, L. Lamaignère, B. Le Garrec, G. Razé, Proc. SPIE 5273 (2004) 312.
[4] L.W. Hrubesh, M.A. Norton, W.A. Molander, E.E. Donohue, S.M. Maricle, B.M. penetrante, R.M. Brusasco, W. Grundler, J.A. Butler, J.W. Carr, R.M. Hill, L.J. Summers, M.D. Feit, A. Rubenchik, M.H. Key, P.J. Wegner, A.K. Burnham, L.A. Hacel, M.R. Kozlowki, Proc. SPIE 4679 (2002) 23.
[5] P. Bouchut, P. Garrec, C. Pelle, Proc. SPIE 4932 (2003) 103.
[6] A.M. Rubenchik, M.D. Feit, Proc. SPIE 4679 (2002) 79.
[7] P. Bouchut, L. Delrive, D. Decruppe, P. Garrec, Proc. SPIE 5273 (2004) 250.
[8] C. Buerhop, B. Blumenthal, R. Weissmann, N. Lutz, S. Biermann, Appl. Surf. Sci. 46 (1990) 430.
[9] M.D. Feit, A.M. Rubenchik, Proc. SPIE 4932 (2003) 91.
[10] J. Zhao, J. Sullivan, T.D. Bennett, Appl. Surf. Sci. 225 (2004) 250.
[11] P.A. Temple, W.H. Lowdermilk, D. Milam, Appl. Opt. 21 (1982) 3249.
[12] R. Brusasco, B. Penetrante, J. Butler, L. Hrubesh, Proc. SPIE 4679 (2002) 40.
[13] K.N. Novak, H.J. Baker, D.R. Hall, Appl. Opt. 45 (2006) 162.
[14] M.A. Stevens-Kalceff, J. Wong, J. Appl. Phys. 97 (2005) 113519.
[15] E. Mendez, K.H. Nowak, H.J. Baker, D.R. Hall, Appl. Opt. 45 (2006) 5358.
[16] M.A. Norton, J.J. Adams, C.W. Carr, E.E. Donohue, M.D. Feit, R.P. Hackel, W.G. Hollingsworth, J.A. Jarboe, M.J. Matthews, A.M. Rubenchik, M.L. Spaeth, Proc. SPIE 6720 (2007) 67200H.
[17] C.W. Carr, M.J. Matthews, J.D. Bude, M.L. Spaeth, Proc. SPIE 6403 (2007) 64030K.
[18] J. Wong, J.L. Ferriera, E.F. Lindsey, D.L. Haupt, I.D. Hutcheon, J.H. Kinney, J. Non-Crystal. Solids 352 (2006) 255.
[19] M. Bass, Laser-materials interactions, in: R. Meyers (Ed.), Encyclopedia of Lasers and Optical Technology, Academic Press, 1991.
[20] Heraeus, Commercial leaflet.
[21] P.A. Temple, W.H. Lowdermilk, D. Milam, Appl. Opt. 42 (1982) 3249.
[22] H. Gong, C. Li, Appl. Opt. 46 (1997) 4954.